Simulation and Verification of the Drop Test of 3C Products

Hsing-Ling Wang[1], Shia-Chung Chen[2], Lei-Ti Huang[2], and Ying Chieh Wang[2]
[1]*Aviation Management Department, Chinese Air Force Academy*
[2]*Mechanical Engineering Department, Chung-Yuan Christian University*

Abstract

Drop test performance has become one of the most crucial evaluations for Computer, Communication, and Consumer (3C) products. Both simulation tool and practical platform for drop test must be established for detailed study. A patented drop test platform is designed for the purpose of impact angle repeatability and instantaneous drop image capture at impact instance. These parameters are two crucial computer-aid-engineering (CAE) inputs used for drop impact simulations. Post data processing procedures such as sampling rate, and signal filtering specifications was also studied and found to be important for the accurate interpretation of drop simulations as well. It was found from simulations that a small angle variation (±5°) may result in up to 36% difference in predicted internal stress. Accurate identification on the impact angle, therefore, is recommended as an important parameter on internal component stress calculation. Good consistency between measured acceleration data and simulated results verifies the practicality of the developed data processing procedure and numerical methodology.

Introduction

The 3C product manufacturers have vastly relied on numerous drop tests to evaluate the robustness of the product structural designs. The evaluation procedure draws more attentions on product survivability from drop test since the impact induced damages, including exterior housing fracture, interior component failure and solder-joint breakage, would have caused huge customer service processing costs [1]. As products designed towards weigh reduction, thin-wall and minified sizes, high impact performance becomes extremely critical for 3C product design issues [1-5]. Conventionally, a product reliability test to prevent impact-induced damage is carried out by a 'design- prototype- test- redesign' procedure. Physical prototype drop test procedures have been performed and verified; however, high cost, time consumption, and lack of analytic information are the major deficiencies. Currently, a commonly employed method for 3C prototype products is the free-fall test; either releasing the test objects by hand [1] or by cutting the strings hung on the 3C products [1-5]. Previous studies indicate that it is difficult to control the orientation of the object at impact in free-hand releasing drop tests, and hence the tests are hard to instrument or repeat. The impact angles could be up to 30° to 40° far from the original releasing orientation [1]. G. Song et al. [5], by using computer simulation method, demonstrates that the variation of impact strain could be different as large as 36% even when the variation of impact angles are merely within 0-4°. Such uncertainties are extremely unfavorable to testing/design engineers since they cannot identify the specific damage mechanism. Therefore, a reliable control on repeatable drop impact angle is very important. Several testing platforms were carried out the with identification feature of impact angle [1-2, 5] and [3-4]. Both platforms utilize high speed camera (HSC) to capture images at the impact instance to confirm the drop impact angle. Although the HSC has a high accuracy to capture the impact instance images, however, its price is too high and the captured image can provides only the projective angle on a single plane rather than the spatial one. As a result, it is necessary to develop a drop test platform with both highly reliable repeatability in impact angle control and image analysis that can accurately determines the drop angle spatially. In addition, the design methodology cannot solely

depend on physical drop tests because it is quite difficult to mount sensors at any desired location internally in a small, compact space to obtain the impact-induced damage information. Computer simulation, on the other hand, is capable to provide more comprehensive mechanical information at any location of interests. If the simulated outputs can be highly correlated with the physical impact information from sensors from a drop test, more impact phenomena can be understood from this validating numerical analysis. Non-linear, transient analytic CAE tools have been widely utilized for verification of product impact performance recently [1-2, 5-6]. A proper modeling of CAE provides an effective methodology to predict structural rigidity during impact. Moreover, the utilization of CAE can eliminate numerous physical drop tests and predict possibilities of structural failure before product manufactured, and, in return, increases the market competition. This study concerns both simulation and physical test for drop impact. This test carrier is a top housing of a Motorola CD938 cellular phone attached with aluminum plate on four boss locations so that overall weight is equal to the weight of a real CD938. A drop test platform developed and patented by Chen, et al. [7-8] was used. The measured acceleration and impact angle derived from the data acquisition system of drop test platform are compared with the outputs from LS-DYNA simulation. A discussion on the correlation between the impact angle variation and maximum stress occurrence are addressed.

FEM and Simulations for CD938

In present study, the drop test carrier is a Motorola CD938 top housing. FEM modeling by LS-DYNA is established for numerical analysis accordingly. Figure 1 shows the meshed model of CD938. Although the CAE simulation does not provide detailed internal stress distribution on some critical parts- like Liquid Crystal Display (LCD) or interconnection parts, current investigation aims at an analytical procedure from this simplified model verification comparing the simulation result with the acceleration sensor output. Parameters utilized in CAE simulation are listed in Table 1. The connections between the aluminum plate and the top housing are 4 spot-weld elements [9]. Possible contact pairs are: top housing vs. rigid table; aluminum plate vs. rigid table; and top housing vs. aluminum plate. The minimum time step, an important parameter that dominates the converging conditions and numerical accuracy for explicit solutions, is automatically determined by LS-DYNA according to the following equation:

$$\Delta t = \Delta k \frac{\Delta l}{C} = \Delta k \frac{\Delta l}{\sqrt{\frac{E}{\rho}}} \tag{1}$$

where it is the smallest time step; *k* is a scaling factor for numerical stability; [10] *l* is the smallest geometric length of the smallest element among the model; C is the elastic wave speed of that material; E is Young's modulus; and ρ is the material density.

Setup of Drop Test Platform

A patented drop test platform [7] is used to monitor the whole drop/impact process, and equipped with data acquisition system and image capturing technology. This drop tester has features of (1) repeatability control of impact angle and (2) accurate identification of drop angle spatially from image captured by CCD. Details can be found elsewhere [8]. An accelerometer is adhered on top of the CD938 housing and calibrated through before test. The impact signal was processed via a computer with amplifier, data acquisition board and A/D converter and all

time-history impulses are then recorded, transformed into actual impact acceleration. The orientation of CD938 upon impact instance is analyzed from the image captured by a CCD and a mirror installed at an inclined angle (45°) to CCD lens [8]. The highest shutter speed of a common CCD can be set to 1/20,000 second and such CCD provides a relative high resolution of drop instance image for spatial angle determination. Table 2 lists the calculated spatial angles from the captured image at drop height of 100 mm. The definition of orientation at impact instance is as follows. Assuming the longitudinal axis of CD938 has a spatial angle along with the global coordinate system, θ_2 is projective angle of this axis on Y-Z plane; and θ_3 is on X-Z plane. The third angle θ_1 on X-Y plane can be calculated by geometric correlation and the spatial orientation of specimen can be determined [7-8].

Comparison and Discussion Between CAE Simulation and Physical Impact Data

Huang [8] gives full description for impact data collection procedures including hardware setup and software monitoring. Sampling rate consideration and frequency filtering specification for simulation results are stated below. Since the impact signal is characterized as low frequency response, a low pass filter following SAE (Society of Automotive Engineer) specification is utilized in current data processing. LS-Post, the post processor of LS-DYNA, provides several signal operating modules such as Fast Fourier Transformation (FFT) and signal filtering schemes which include SAE, Butterworth and FIR specifications [9]. By converting the impact, time-domain signals derived from accelerometer into frequency domain through FFT, the cut-off frequency of 1200 Hz is chosen because the rest responses are quickly decayed after this index. (Figure 2) In order to eliminate high frequency noises, current study applies SAE CFC 710 [10] as low-pass filtering specification for those signals derived from both accelerometer and numerical simulation. The sampling rate is 30,000 Hz and is twice far beyond the cut-off frequency to avoid any aliasing phenomenon. The accelerometer is a PCB Model 352C22 and weighs 0.5 grams (0.6% of total weight of test carrier: 79.73 grams). The weight ratio of accelerometer to the test carrier is limited within 10%, and maximum measuring impact acceleration is 500g (1g=0.00981 mm/ms^2). The nodal acceleration output is the average outputs from several nodes in order to level off the local mass concentration effect of accelerometer and is filtered following SAE CFC710 specification. Impact acceleration, compared between the physical impact signal and numerical results from LS-DYNA, is shown in Figure 3. The highly agreement between these two curves indicates that this signal filtering procedure is quite accurate (Table 3). The stress simulation results are shown in Figure 4 and 5. No surprisingly, the impact contact area is the highest stress occurrence location. By presenting the stress wave in propagating contour plots, the earliest wave front is appearing at Boss#1 (2.333 ms after impact) where the heavy aluminum panel hangs on this connection point. The impact stress wave is then traveling along the aluminum plate and Boss#2 emerges stress wave 0.033 ms after Boss#1 is impacted. (2.367 ms after impact, Figure 6) The stress wave propagates longitudinally (along aluminum panel) to the top two Bosses at 3.333 ms after impact. (Figure 7) By examining the specimens after impact, the boss locations on CD938 plastic housing show emulsified color, which indicates that those spots had experienced serious energy shock. That shock effect gives clear explanation since those connection spots are usually the critical points of part failure.

Figure 8 is the stress plot at location of BOSS1 vs. impact duration, and Table 4 shows the maximum stress of BOSS1 at different impact angle. For example, the maximum stress is 20.8

MPa as θ = 32°. The variation of θ_2 is the inclined angle of longitudinal axis of CD938 on the projective YZ plane (Figure 9). Therefore, a smaller θ_2 indicates that CD938 is closer to direct impact. (No inclined angle on projective YZ plane) If the impact angle is controlled within ±3°(32°±3° or 29°~35°), the absolute maximum stresses difference at BOSS1, compared with the 20.8 MPa as θ = 32°, is only within 10% (0.48%~8.19%). However, if the variation goes to ±5°(32°±5° or 27°~37°), the absolute maximum stresses difference can be as large as 34% (34.6%; θ=27°). As θ becomes smaller, the CD938 is declined to direct impact, as no double, the impact stress increases. Same analytical procedure is applied on the variation of θ, the angle varies from 18°±5° (13° to 23°) as θ is fixed at 32° (Figure 9). Table 5 summarizes the impact stress variation vs. impact angle, and shows more discrepant in maximum stress even the angle variation is only within ±3° (15.8% to 26.0%). This numerical result is similar to the conclusion of Reference 5, and confirms the importance of impact angle control in a physical drop test. If the impact angle cannot be well controlled within specific range, (e.g. within ±3°) the predicted internal stress may be different by as high as 30%. It may also lead to a wrong conclusion in that the predicted failure location shows unexpected failure pattern from physical drop test. Moreover, repeated physical drop tests show meaningless consequences if the impact angle is uncontrollable.

Conclusions

1. A drop test platform with impact angle control repeatability and analysis capability has been developed. Excellent control on impact angle provides product engineers a better understanding on the failure pattern of specific drop orientation and the damage mechanism of structures.
2. Numerical simulation provides stress wave propagating directions within internal components, where it is unlike to mount any mechanical sensors in a compact space of 3C products. Current study uses a simple specimen to compare the physical acceleration and simulation results with relatively good accuracy. The simulation procedure of this simplified specimen provides the knowledgeable information on impact simulation when a more complicated 3C product is applied.
3. A proper filtering technology is crucial to remove unrelated high frequency noises during impact test. A low pass filter following SAE specification proves to be useful and filtered curves of both experimental data and simulation outputs present an easier understanding of those signals.

Acknowledgements

Current study is sponsored by National Science Council (grant number NSC-91-2212-E-013-006) and the distinguished research grant of Chung Yuan Christian University.

Reference

1. J. Wu, et al., (1996), “Drop/Impact Simulation of Electronic Product”, 4th International LS-DYNA3D Conference, Minneapolis, MN, September 6.
2. J. Wu, G. Song, C.P. Yeh,, K. Wyatt, (1998), “Drop/Impact Simulation and Test Validation of Telecommunication Products”, Inter. Society Conference on Thermal Phenomena, pp. 330-336.
3. S. Goyal, S. Upasani, and D.M. Patel, (1999), “Improving Impact Tolerance of Portable Electric Products: Case Study of Cellular Phones”, Experimental Mechanics, 39, 43~52.

4. S. Goyal, (2000), "Methods for Realistic Drop-Testing", International Journal of Microcircuits and Electronic Packaging, 23, 45-52.
5. G. Song, C.P. Yeh, and L. Wyatt, (1999), "Phone Drop Simulation and Effect of Small Variations of Drop Angle", Proceeding of the 1999 Winter Motorola AMT Symposium.
6. C. T. Chang, S. C. Chen, J. P. Chen, H. S. Peng, and L. T. Huang, (2000), "Drop-Impact Simulations of a 3C Thin-Wall Part", 24th National Conference on Applied and Theoretical Mechanics, Taiwan, R.O.C., pp. Q108-115.
7. S. C. Chen, L. T. Huang, C. C. Chou, W. I. Kuo, and C. H. Shih, (2003) "Detecting method of a drop test and the device thereof". Patent pending, filed on 8 April, 2003.
8. L. T. Huang, (2003), Study on the drop test of thin-wall product, Ph.D. Thesis, June.
9. J. O. Hallquist, (1998), "LS-DYNA Theoretical Manual", Livermore Software of Technology Corporation, May.
10. E. L. Fasanella and K. E. Jackson, (2002), "Best Practices for Crash Modeling and Simulation" NASA/TM-2002-211944 ARL-TR-2849

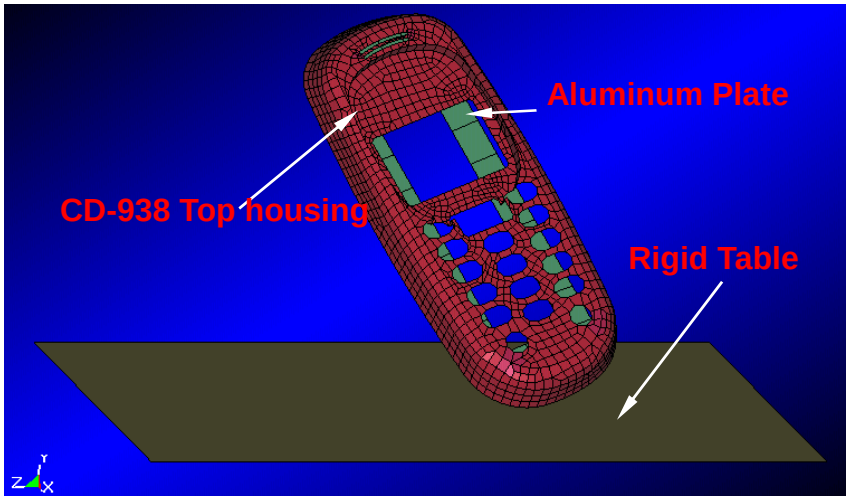

Figure 1. Finite element model of CD938 (LS-DYNA)

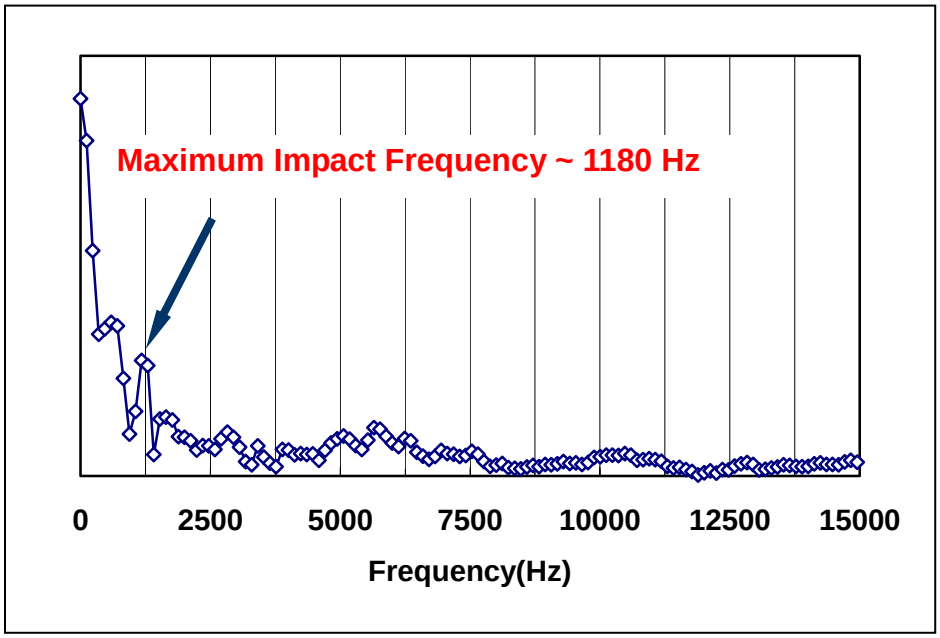

Figure 2. LS-Post FFT curve from experimental impact acceleration data

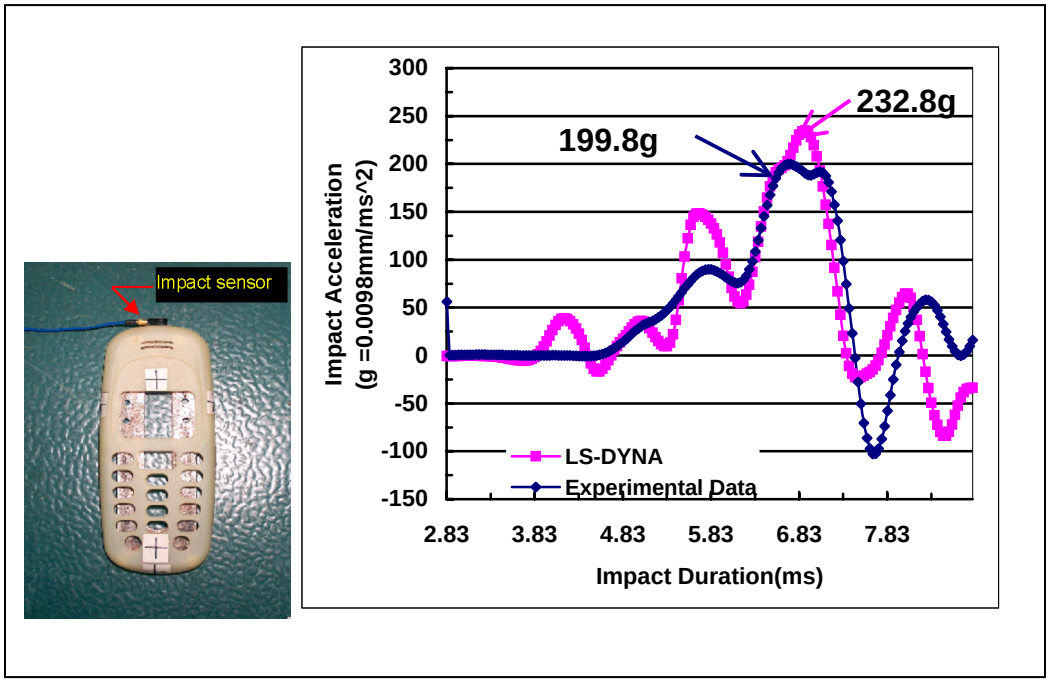

Figure 3. Comparison between experimental data with simulation results (Acceleration)

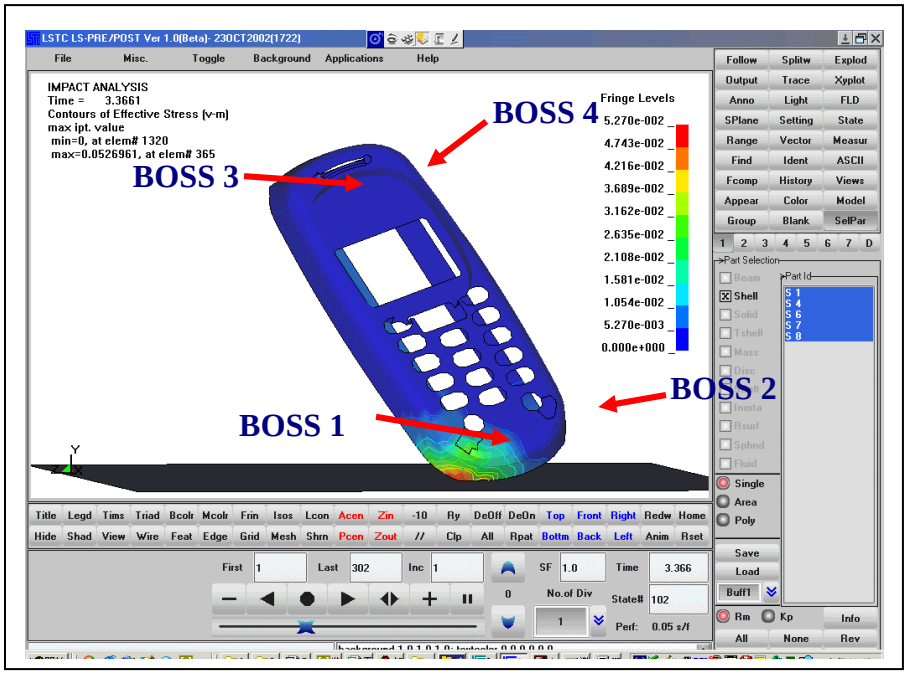

Figure 4. Maximum impact stress

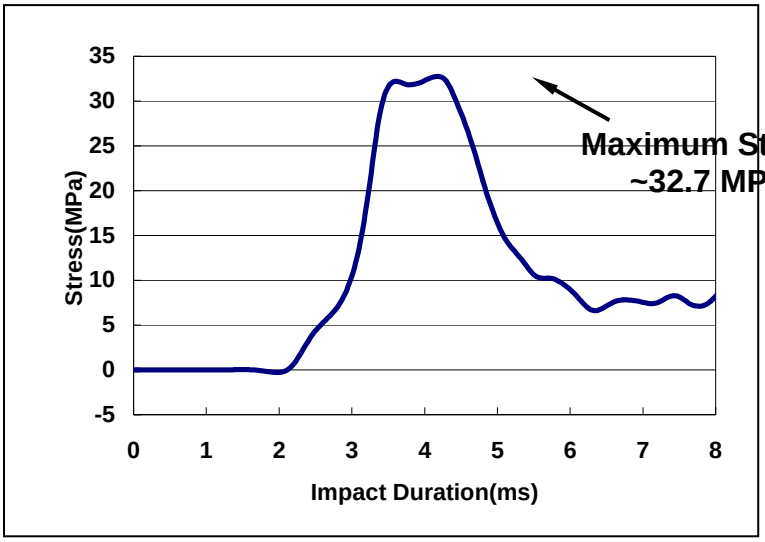

Figure 5. Impact stress historical plot of the first contact area.

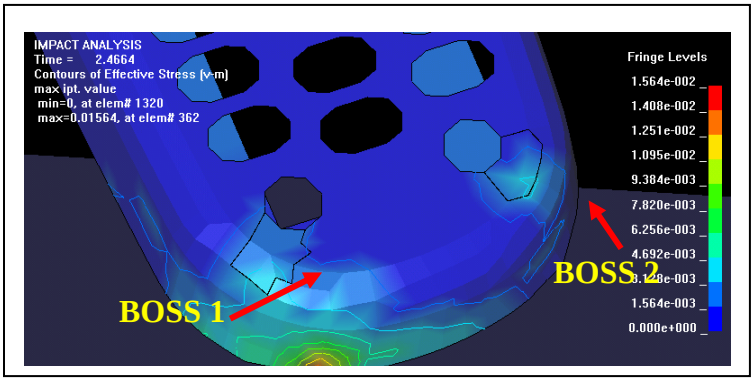

Figure 6. Stress wave propagating patterns (BOSS 1,2)

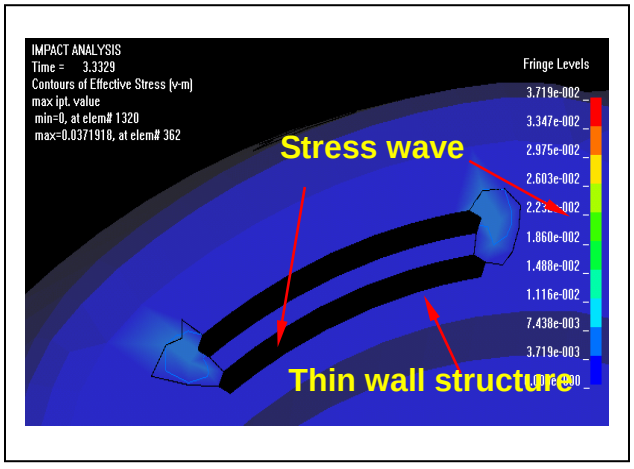

Figure 7. Stress wave propagating patterns and thin wall structure (BOSS 3,4)

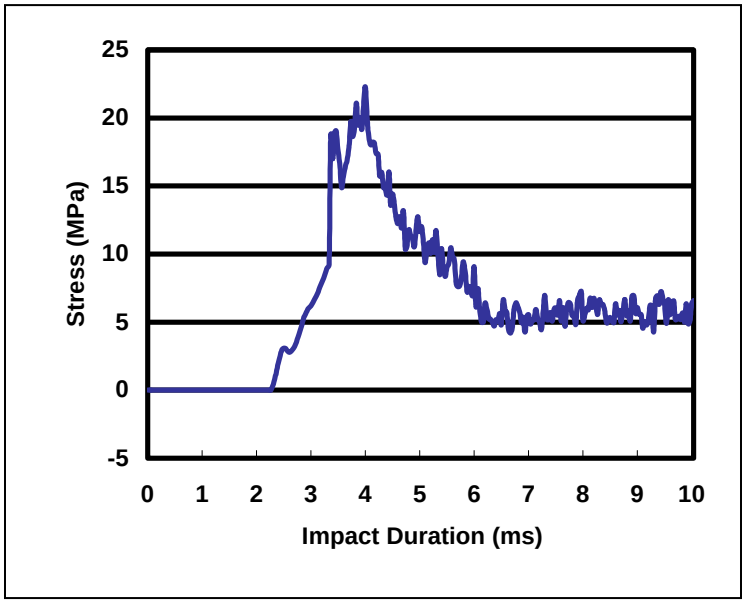

Figure 8. Impact Stress at BOSS 1

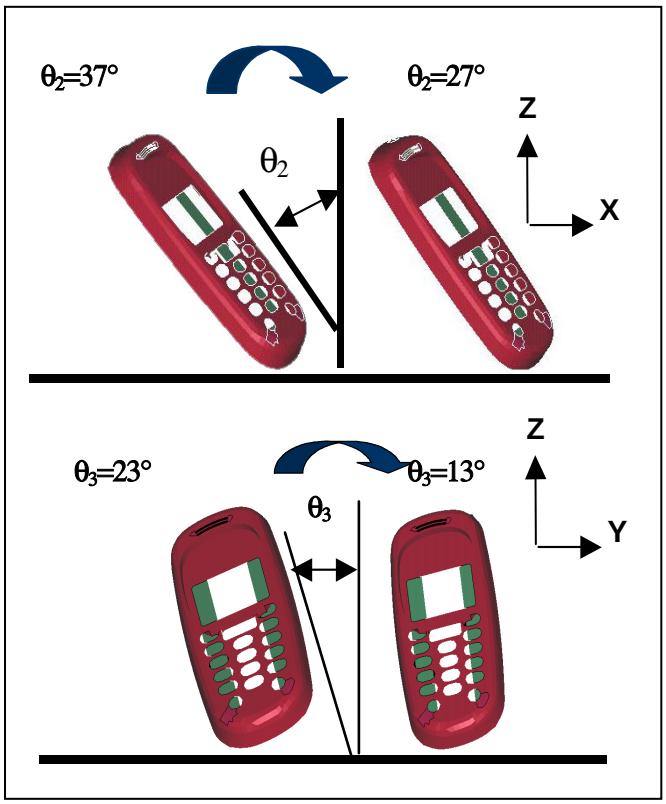

Figure 9. Impact angle variation in θ_2 and θ_3

Table 1 CD938 finite element modeling properties

Part	Weigh (gram)	E (Gpa)	σ_y (Mpa)	ν	Thickness (mm)	Ele.#
Top housing Shell	7.74	2.60	43.20	0.380	0.7	1320
Aluminum Plate Shell	71.97	70.0	323.8	0.334	3.34	75
Spot Weld						4
Rigid Table		210.0	248.0	0.334	1.0	1

Table 2. CD938 drop test parameters

Drop Height (H)	100 mm	Impact angle	Degree°
		Plane Y-Z (Meas.)	$\theta_3 = 18°$
Velocity at impact instance $V=\sqrt{(2\ g\ H)}$ $g= 0.0098\ mm/ms^2$	1.4 mm/ms	Plane X-Z (Meas.)	$\theta_2 = 32°$
		Plane X-Y (Calcu.)	23°

Table 3. Impact accelerations

	Measured	FEM
Impact acceleration $g = 0.0098mm/ms^2$	199.8 g	232.8 g

Table 4. Max. Stress vs. Impact angle (θ_2=32°)

Impact Angle	Max. Stress (MPa)	Absolute Difference (%)
27°	28.0	34.6%
28°	22.6	8.7%
29°	21.6	3.8%
30°	22.5	8.2%
31°	20.7	0.5%
32°	20.8	0.00%
33°	19.6	5.8%
34°	20.0	3.8%
35°	20.8	0.0%
36°	21.2	1.9%
37°	22.4	7.7%

Table 5. Max. Stress vs. Impact angle (θ_3=18°)

Impact Angle	Max. Stress (MPa)	Absolute Difference (%)
13°	15.06	27.6%
14°	15.05	27.6%
15°	15.39	26.0%
16°	15.80	24.0%
17°	19.20	7.7%
18°	20.80	0.0%
19°	21.57	3.7%
20°	23.11	11.1%
21°	24.09	15.8%
22°	25.39	22.1%
23°	25.91	24.6%